Inorganic Chemistry

Article

pubs.acs.org/IC

Series of Mixed Uranyl–Lanthanide (Ce, Nd) Organic Coordination Polymers with Aromatic Polycarboxylates Linkers

Ionut Mihalcea, Christophe Volkringer, Natacha Henry, and Thierry Loiseau*

Unité de Catalyse et Chimie du Solide (UCCS)–UMR CNRS 8181, Université de Lille Nord de France, USTL-ENSCL, Bat C7, BP 90108, 59652 Villeneuve d'Ascq, France

Supporting Information

ABSTRACT: Three series of mixed uranyl-lanthanide (Ce or Nd) carboxylate coordination polymers have been successfully synthesized by means of a hydrothermal route using either conventional or microwave heating methods. These compounds have been prepared from mixtures of uranyl nitrate, lanthanide nitrate together with phthalic acid (**1**,**2**), pyromellitic acid (**3**,**4**), or mellitic acid (**5**,**6**) in aqueous solution. The X-ray diffraction (XRD) single-crystal revealed that the phthalate complex $(UO_2)_4O_2Ln(H_2O)_7(1,2\text{-bdc})_4{\cdot}NH_4{\cdot}xH_2O$ (Ln = Ce(**1**), Nd(**2**); x = 1 for **1**, x = 0 for **2**), is based on the connection of tetranuclear uranyl-centered building blocks linked to discrete monomeric units $LnO_2(H_2O)_7$ via the organic species to generate infinite chains, intercalated by free ammonium cations. The pyromellitate phase $(UO_2)_3Ln_2(H_2O)_{12}(btec)_3{\cdot}5H_2O$ (Ce(**3**), Nd(**4**)) contains layers of monomeric uranyl-centered hexagonal and pentagonal bipyramids linked via the carboxylate arms of the organic molecules. The three-dimensionality of the structure is ensured by the connection of remaining free carboxylate groups with isolated monomeric units $LnO_2(H_2O)_7$. The network of the third series $(UO_2)_2(OH)Ln(H_2O)_7(mel){\cdot}5H_2O$ (Ce(**5**), Nd(**6**)) is built up from dinuclear uranyl units forming layers through connection with the mellitate ligands, which are further linked to each other through discrete monomers $LnO_3(H_2O)_6$. The thermal decomposition of the various coordination complexes led to the formation of mixed uranium-lanthanide oxide, with the fluorite-type structure at 1500 °C (for **1**, **2**) or 1400 °C for **3**–**6**. Expected U/Ln ratio from the crystal structures were observed for compounds **1**–**6**.

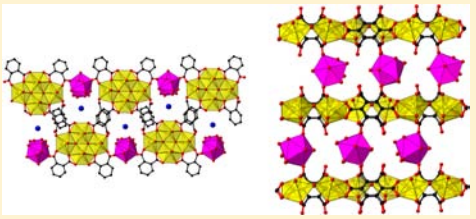

INTRODUCTION

The formation of coordination polymers involving actinide cations with O-donor organic ligands (i.e., multidentate carboxylates) has been extensively investigated in the past decades, especially with hexavalent uranium.[1] A large number of hybrid organic–inorganic architectures have thus been reported with different dimensionalities, exhibiting various coordination states (six-, seven-, or eight-fold) for uranyl cations together with diverse building units from isolated mononuclear up to octanuclear motifs or infinite chain-like nets. For the organic part, the reactivity of aliphatic[2] or aromatic[2d,f,3] polycarboxylate has been explored and successfully led to the so-called uranyl-organic frameworks (UOFs). The association of a hetero metal such as rare-earth element was rarely reported in literature and was, for instance, recently described by Thuéry[4] and our group.[5] This is quite a challenging task since the mixture of the 4f and 5f elements commonly leads to the segregation of coordination complexes containing separately each metallic cation. One strategy could consist in using organic linkers with appropriate functionalities (ex N- or/and O-donor), which offer preferential interactions toward actinide or lanthanides. Several mixed 4f-5f complexes have thus been isolated so far.[6] Concerning the carboxylate-type ligand, the illustrations of uranyl-lanthanide organic assemblies are still rare.[4,5,7] However, heterometallic 4f-5f phosphonates involving Ce[8] or Sm[9] or sulfonates with Nd, Dy, Er, Yb[10] and uranyl cations have been also recently reported, with direct U–O–Sm bonding associated in the case of the phosphonoacetate group.[9] From the industrial point of view, the chemical interaction of lanthanide with uranium is of important interest since both elements are present after using uranium oxide (UO_2) in a nuclear reactor, and thus found after nitric acid dissolution in aqueous solution for its recycling process.

In this context, the reactivity of uranium and cerium or neodymium has been investigated with various multidentate carboxylic acids such as phthalic acid (noted 1,2-H_2bdc), pyromellitic acid (noted H_4btec), and mellitic acid (noted H_6mel). By using the hydrothermal synthesis route, different novel coordination complexes have been isolated with the polytopic carboxylate groups complexing both uranyl and lanthanide cations. The present contribution describes the preparation and crystal structures of three series of compounds, $(UO_2)_4O_2Ln(H_2O)_7(1,2\text{-bdc})_4{\cdot}NH_4{\cdot}xH_2O$ (Ln = Ce(**1**), Nd(**2**); x = 1 for **1**, x = 0 for **2**), $(UO_2)_3Ln_2(H_2O)_{12}(btec)_3{\cdot}5H_2O$ (Ce(**3**), Nd(**4**)) and $(UO_2)_2(OH)Ln(H_2O)_7(mel){\cdot}5H_2O$ (Ce(**5**), Nd(**6**)). As previously reported,[4] the parameters controlling the hydrothermal synthesis of mixed 4f-5f coordination complexes were quite delicate to handle to get pure solids. Particularly, some difficulties appeared for the

Received: March 20, 2012
Published: August 29, 2012

   dx.doi.org/10.1021/ic3005757 | *Inorg. Chem.* 2012, 51, 9610–9618

preparation of the phases **1** and **2**, for which mixtures of compounds were formed during reactions by using conventional electrical heating system. Another possible alternative is the utilization of microwave heating method, which has been successfully applied to the preparation of MOF-type materials[11] or coordination complexes.[12] This technique was tested for compounds **1** and **2**, which favored its crystallization as pure phase. Their thermal decomposition was then analyzed by X-ray diffraction, which showed the decomposition into $(U,Ln)O_2$ oxide with the structural fluorite type.

EXPERIMENTAL SECTION

Synthesis. ***Caution!*** *While uranyl nitrate $UO_2(NO_3)_2{\cdot}6H_2O$ is a radioactive and chemically toxic reactant, precautions with suitable care and protection for handling such substances have been followed.*

The coordination complexes have been hydrothermally synthesized under autogenous pressure using a 23 mL Teflon-lined stain-less steel Parr autoclave from the following reactants: cerium nitrate hexahydrate ($Ce(NO_3)_3{\cdot}6H_2O$, Aldrich, 99%), neodymium nitrate hexahydrate ($Nd(NO_3)_3{\cdot}6H_2O$, Aldrich, 99.9%), uranyl nitrate hexahydrate ($UO_2(NO_3)_2{\cdot}6H_2O$, Merck 99%), phthalic acid ($C_6H_4(CO_2H)_2$, 1,2-benzenedicarboxylic acid or 1,2-H_2bdc, Acros Organics, 99%), pyromellitic acid ($C_6H_2(CO_2H)_4$, 1,2,4,5-benzenetetracarboxylic acid or H_4btec, Aldrich 96%), mellitic acid ($C_6(CO_2H)_6$, 1,2,3,4,5,6-benzenehexacarboxylic acid or H_6mel, Aldrich, 99%), ammonia solution (Prolabo, 28%), sodium hydroxide (NaOH, Aldrich, 98%), and deionized water. The starting chemical reactants are commercially available and have been used without any further purification.

*$(UO_2)_4O_2Ce(H_2O)_7(1,2\text{-}bdc)_4{\cdot}NH_4{\cdot}H_2O$ (**1**).* A mixture of 508 mg of (1 mmol) $UO_2(NO_3)_2{\cdot}6H_2O$, 614 mg of (1.4 mmol) $Ce(NO_3)_3{\cdot}6H_2O$, 0.16 mL of (0.97 mmol) phthalic acid, 1.8 mL of (3.6 mmol) NH_3 (2M), and 3.0 mL of (167 mmol) H_2O was placed in a Parr autoclave and then heated statically at 150 °C for 24 h (final pH = 2.9). The resulting product of **1** was then filtered off, washed with water, and dried at room temperature. For unknown reasons, the use of this procedure led to irreproducible and random results. X-ray diffraction (XRD) analyses indicated the presence of multiple phases for these samples. Compound **1** could be obtained as pure phase (from XRD analyses) by means of microwave assisted heating (oven CEM Mars) from a mixture of 508 mg of (1 mmol) $UO_2(NO_3)_2{\cdot}6H_2O$, 614 mg of (1.4 mmol) $Nd(NO_3)_3{\cdot}6H_2O$, 0.16 mL of (0.97 mmol) phthalic acid, 1.6 mL of (3.2 mmol) NH_3 (2M), and 8.4 mL of (467 mmol) H_2O at 150 °C for 2 h (final pH = 2.6). Scanning electron microscopy (SEM) examination indicated that crystal size differed from the two heating methods. One observed isolated crystallites of 100−500 μm size by reaction using conventional electrical heating whereas the isolated crystallites had 30−100 μm size by using microwave heating (Supporting Information, Figure S1a).

*$(UO_2)_4O_2Nd(H_2O)_7(1,2\text{-}bdc)_4{\cdot}NH_4$ (**2**).* A mixture of 254 mg of (0.5 mmol) $UO_2(NO_3)_2{\cdot}6H_2O$, 310 mg of (0.7 mmol) $Nd(NO_3)_3{\cdot}6H_2O$, 0.08 mL of (0.49 mmol) phthalic acid, 0.8 mL of (1.6 mmol) NH_3 (2M), and 4.2 mL of (233 mmol) H_2O was placed in a Parr autoclave and then heated statically at 200 °C for 24 h (final pH = 3.5). The resulting product of **2** was then filtered off, washed with water, and dried at room temperature. For unknown reasons, the use of this procedure led to irreproducible and random results. XRD analyses indicated the presence of multiple phases for these samples. Compound **2** could be obtained as pure phase (from XRD analyses) by means of microwave assisted heating (oven CEM Mars) from a mixture of 508 mg of (1 mmol) $UO_2(NO_3)_2{\cdot}6H_2O$, 620 mg of (1.4 mmol) $Nd(NO_3)_3{\cdot}6H_2O$, 620 mg of (1.4 mmol) phthalic acid, 1.6 mL of (3.2 mmol) NH_3 (2M), and 8.4 mL of (467 mmol) H_2O at 150 °C for 2 h (final pH = 3.5). SEM examination indicated that crystal size differed from the two heating methods. One observed crystalline agglomerates of 150−400 μm size by reaction using conventional electrical heating whereas the single crystallites had 50−250 μm size by using microwave heating (Supporting Information, Figure S1a). For compounds **1** and **2**, we observed the formation of well-defined and multifaceted crystallites in the case of microwave heating whereas the particles contained agglomerated crystallites in the case of conventional electrical heating. The difference of crystal growth behavior could result from the very fast kinetics of nucleation occurring under microwave irradiation, which prevents the growth of large crystals in some cases.[11b,13]

*$(UO_2)_3Ce_2(H_2O)_{12}(btec)_3{\cdot}5H_2O$ (**3**).* A mixture of 508 mg of (1 mmol) $UO_2(NO_3)_2{\cdot}6H_2O$, 351 mg of (0.8 mmol) $Ce(NO_3)_3{\cdot}6H_2O$, 132 mg of (0.5 mmol) pyromellitic acid, 1.2 mL of (2.4 mmol) NH_3 (2M), and 3.8 mL of (211 mmol) H_2O was placed in a Parr autoclave and then heated statically at 150 °C for 24 h (final pH = 2.7). The resulting product was then filtered off, washed with water and dried at room temperature. SEM examination indicated platelet-like elongated crystallites (Supporting Information, Figure S1b).

*$(UO_2)_3Nd_2(H_2O)_{12}(btec)_3{\cdot}5H_2O$ (**4**).* A mixture of 502 mg of (1 mmol) $UO_2(NO_3)_2{\cdot}6H_2O$, 442 mg of (1 mmol) $Nd(NO_3)_3{\cdot}6H_2O$, 132 mg of (0.5 mmol) pyromellitic acid, 1.2 mL of (2.4 mmol) NH_3 (2M), and 3.8 mL of (211 mmol) H_2O was placed in a Parr autoclave and then heated statically at 150 °C for 6 h (final pH = 1.9). The resulting product was then filtered off, washed with water and dried at room temperature. SEM examination indicated platelet-like crystallites (Supporting Information, Figure S1b).

*$(UO_2)_2(OH)Ce(H_2O)_7(mel){\cdot}5H_2O$ (**5**).* A mixture of 502 mg of (1 mmol) $UO_2(NO_3)_2{\cdot}6H_2O$, 100 mg of (0.4 mmol), $Ce(NO_3)_3{\cdot}6H_2O$, 85 mg of (0.25 mmol) mellitic acid, 5 mL of (277 mmol) H_2O, and 0.3 mL of (1.2 mmol) NaOH (4M) was placed in a Parr autoclave and then heated statically at 150 °C for 4 h (final pH = 1.8). The resulting product was then filtered off, washed with water, and dried at room temperature. SEM examination indicated platelet-like crystallites (Supporting Information, Figure S1c).

*$(UO_2)_2(OH)Nd(H_2O)_7(mel){\cdot}5H_2O$ (**6**).* A mixture of 502 mg of (1 mmol) $UO_2(NO_3)_2{\cdot}6H_2O$, 200 mg of (0.25 mmol), $Nd(NO_3)_3{\cdot}6H_2O$, 85 mg of (0.25 mmol) mellitic acid, 5 mL of (277 mmol) H_2O, and 0.1 mL of (0.4 mmol) NaOH (4M) was placed in a Parr autoclave and then heated statically at 150 °C for 24 h (final pH = 0.9). The resulting product showing was then filtered off, washed with water, and dried at room temperature. SEM examination indicated platelet-like crystallites (Supporting Information, Figure S1c).

Single-Crystal X-ray diffraction. Crystals were easily selected under polarizing optical microscope and glued on a glass fiber for a single-crystal X-ray diffraction experiment. X-ray intensity data were collected on a Bruker X8-APEX2 CCD area-detector diffractometer using Mo-K_α radiation (λ = 0.71073 Å) with an optical fiber as collimator. Several sets of narrow data frames (20 s per frame) were collected with ω scans. Data reduction was accomplished using SAINT V7.53a.[14] The substantial redundancy in data allowed a semiempirical absorption correction (SADABS V2.10[15]) to be applied, on the basis of multiple measurements of equivalent reflections. The structure was solved by direct methods, developed by successive difference Fourier syntheses, and refined by full-matrix least-squares on all F data using the JANA2006[16] program. The final refinements included anisotropic thermal parameters of all non-hydrogen atoms. For compound **3**, the refinement results gave rise to a largest Fourier difference peak 17.4 e Å^{-3} at 0.7 Å around the Ce atom with a reliability factor of 0.0454. To check a possible structural disorder, a Maximum Entropy Method (MEM) analysis of the diffraction data was carried out using the program BAYMEM.[17] The unit cell was divided into a grid of 72 × 72 × 486 pixels to ensure a good spatial resolution (the reliability factor of the MEM equal to 1.8). The visualized three-dimensional electron density (ED) images (shown in Supporting Information, S2) using Vesta software,[18] clearly showed that the electron density around the Ce site broadened with a pear form indicating that the cation is distributed over two split sites with different weights. So, two Ce atoms with respectively 0.8 and 0.2 occupancies were introduced in the calculation procedure and then the occupancies have been refined to the values 0.875(2)/0.125(2) with the constraint of unity. Their U_{iso} parameters were fixed to be equal. No disorder for the oxygen atoms around the two cerium atoms have been observed on the electron density images, this can be explained by the low occupancy of the

dx.doi.org/10.1021/ic3005757 | Inorg. Chem. 2012, 51, 9610−9618

Table 1. Crystal Data and Structure Refinements for Mixed Uranyl-Lanthanide (Ce, Nd) Carboxylates

	1	2	3	4	5	6
formula	$C_{32}H_{16}CeNO_{34}U_4$	$C_{32}H_{16}NNdO_{33}U_4$	$C_{30}H_6Ce_2O_{47}U_3$	$C_{30}H_6Nd_2O_{47}U_3$	$C_{12}CeO_{29}U_2$	$C_{12}NdO_{29}U_2$
formula weight	2050.7	2038.8	2112.7	2120.9	1224.3	1228.4
temperature/K	293(2)	293(2)	293(2)	293(2)	293(2)	293(2)
crystal type	yellow block	yellow block	purple block	purple block	yellow platelet	yellow needle
crystal size/mm	0.12 × 0.08 × 0.05	0.17 × 0.07 × 0.06	0.15 × 0.11 × 0.07	0.15 × 0.13 × 0.03	0.13 × 0.08 × 0.02	0.21 × 0.20 × 0.08
crystal system	monoclinic	monoclinic	triclinic	triclinic	orthorhombic	orthorhombic
space group	$P2/n$	$P2/n$	$P\bar{1}$	$P\bar{1}$	$Pna2_1$	$Pna2_1$
a/Å	15.9635(2)	15.9634(6)	10.9229(2)	10.8981(13)	15.8523(8)	15.8367(8)
b/Å	19.9741(3)	19.9848(8)	11.5371(3)	11.5452(14)	8.3188(5)	8.3203(6)
c/Å	7.2160(1)	7.1993(3)	13.4516(3)	13.4086(16)	21.5884(12)	21.5047(3)
α/deg	90	90	69.5020(5)	69.399(3)	90	90
β/deg	95.3854(7)	95.430(2)	80.0490(6)	79.959(3)	90	90
γ/deg	90	90	62.2530(5)	62.242(2)	90	90
volume/Å^3	2289.63(5)	2286.5(2)	1405.14(6)	1397.4(3)	2846.9(3)	2833.6(3)
Z, $\rho_{calculated}$/g cm^{-3}	2, 2.974	2, 2.960	1, 2.496	1, 2.520	4, 2.856	4, 2.879
μ/mm^{-1}	15.182	15.34	10.318	10.604	13.036	13.323
Θ range/deg	1.02 − 26.52	1.64 − 26.4	1.62 − 30.98	1.62 − 32.58	1.89 - 33.72	2.57 - 30.56
limiting indices	$-19 \le h \le 19$	$-19 \le h \le 19$	$-15 \le h \le 15$	$-16 \le h \le 16$	$-24 \le h \le 24$	$-20 \le h \le 22$
	$-24 \le k \le 24$	$-24 \le k \le 24$	$-16 \le k \le 16$	$-17 \le k \le 17$	$-12 \le k \le 12$	$-11 \le k \le 11$
	$-9 \le l \le 9$	$-9 \le l \le 8$	$-19 \le l \le 19$	$-20 \le l \le 20$	$-33 \le l \le 31$	$-28 \le l \le 30$
collected reflections	31635	52752	37593	47359	58532	26709
unique reflections	4673	22816	8899	10168	10922	8088
	[R(int) = 0.0356]	[R(int) = 0.079]	[R(int) = 0.0352]	[R(int) = 0.0485]	[R(int) = 0.0687]	[R(int) = 0.0517]
parameters	310	306	364	365	337	191
goodness-of-fit on F^2	3.80	1.35	2.38	1.62	1.25	1.00
final R indices [$I > 2\sigma(I)$]	R1 = 0.0594	R1 = 0.0561	R1 = 0.0332	R1 = 0.0304	R1 = 0.0365	R1 = 0.0313
	wR2 = 0.0793	wR2 = 0.0562	wR2 = 0.0500	wR2 = 0.0418	wR2 = 0.0375	wR2 = 0.0351
R indices (all data)	R1 = 0.0694	R1 = 0.1507	R1 = 0.0380	R1 = 0.0456	R1 = 0.0612	R1 = 0.0443
	wR2 = 0.0799	wR2 = 0.0789	wR2 = 0.0505	wR2 = 0.0430	wR2 = 0.0400	wR2 = 0.0375
largest diff. peak and hole/e Å^{-3}	6.37 and −5.93	3.21 and −1.92	5.77 and −4.00	2.10 and −1.98	2.-91 and −2.23	1.50 and −1.35

Ce1b = 0.125(2). The refinements led to the $R1$ values of 0.0332 for this structural model. The crystal data of the six compounds **1**−**6** are given in Table 1. Supporting Information is available in CIF format.

Thermogravimetric Analysis. The thermogravimetric experiments have been carried out on a thermoanalyser TGA 92 SETARAM under air atmosphere with a heating rate of 5 °C.min^{-1} from room temperature up to 800 °C. X-ray thermodiffractometry was performed under 5 L·h^{-1} air flow in an Anton Paar HTK1200N of a D8 Advance Bruker diffractometer (θ−θ mode, CuKα radiation) equipped with a Vantec1 linear position sensitive detector (PSD). Each powder pattern was recorded in the range 5−60° (2θ) (at intervals of 20 °C up to 800 °C) with a 0.5 s/step scan, corresponding to an approximate duration of 30 min. The temperature ramps between two patterns were 0.08 °C·s^{-1} up to 800 °C. Calcinations of the mixed uranyl-lanthanide compounds at higher temperatures such as 1400 (**3**−**6**) or 1500 °C (**1**−**2**) have been carried out in a furnace, by using platinum crucibles and following a thermal treatment of 24 h under air atmosphere.

Infrared Spectroscopy. Infrared spectra of compounds **1**−**6** were measured on Perkin-Elmer Spectrum Two spectrometer between 4000 and 400 cm^{-1}, equipped with a diamond Attenuated Total Reflectance (ATR) accessory (see Supporting Information).

Fluorescence. Fluorescence spectra of the powdered compounds **1**−**6** were measured at room temperature on SAFAS FLX-Xenius spectrometer between 440 and 620 nm, equipped with a xenon lamp. The fluorescence spectrum of uranyl dinitrate hexahydrate, $UO_2(NO_3)_2{\cdot}6H_2O$, was also presented for comparison. The resulting spectra were quite complex for direct interpretation and only the list of main bands are provided (see Supporting Information).

RESULTS

Structure Description. *Crystal Structure of $(UO_2)_4O_2Ln(H_2O)_7(1,2\text{-bdc})_4{\cdot}NH_4{\cdot}xH_2O$ (Ln = Ce(1), Nd(2); x = 1 for **1**, x = 0 for **2**).* The compounds **1** and **2** exhibit a similar structure consisting of three crystallographically independent uranium atoms and one lanthanide atom (Figure 1). Two of the uranium centers (U1 and U2, special position *2f*) adopt an 8-fold coordination (hexagonal bipyramid) whereas the third one (U3, position *4g*) has a 7-fold coordination (pentagonal bipyramid). For these three cations, terminal short U−O bondings are observed with U−O distances in the range 1.719(9)−1.779(2) Å for **1** and 1.760(6)−1.764(6) Å for **2**, which are typical of the double uranyl bond, commonly found for hexavalent uranium. The U−O distances involved in the equatorial plane range from 2.241(9) up to 2.636(9) Å (**1**) and 2.241(6) up to 2.629(6) Å (**2**) for U1 and U2, from 2.196(11) up to 2.414(9) Å (**1**) and 2.192(6) up to 2.379(6) Å (**2**) for U3. The two hexagonal bipyramids (U1 and U2) are edge-shared through the oxygen atom O1. The latter also bridges the third uranyl center U3, showing a μ_3-connection mode. Valence bond calculations[19] give the values of 2.10 (**1**) and 2.09 (**2**) for O1 and agree with the occurrence of an oxo group. U3-centered polyhedron also shares a common edge with U1 and U2, via the second oxo groups O81a or O81b. These two oxygen atoms also belong to one of the two carboxylate arms of the phthalate species and therefore adopt a μ_3-connection fashion. The edge-sharing mode occurring between the three uranyl-centered polyhedra gives rise to the formation of a

dx.doi.org/10.1021/ic3005757 | Inorg. Chem. 2012, 51, 9610−9618

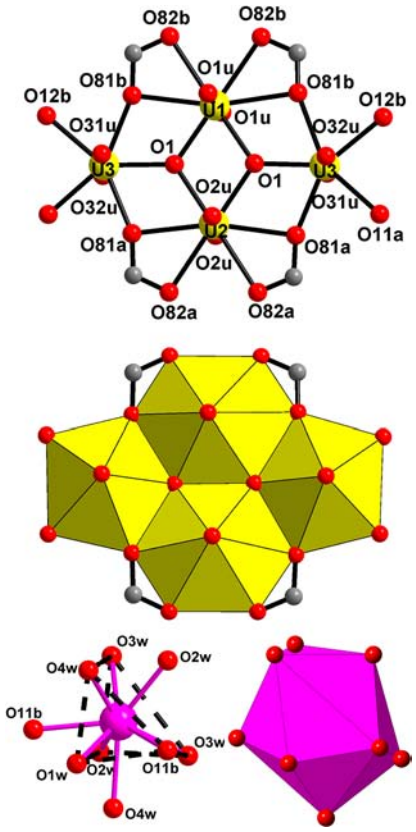

Figure 1. Structure of $(UO_2)_4O_2Ln(H_2O)_7(1,2\text{-bdc})_4{\cdot}NH_4{\cdot}xH_2O$ (Ln = Ce(**1**), Nd(**2**); x = 1 for **1**, x = 0 for **2**)). (top) View of the tetrameric asymmetric unit involving uranyl centers. (bottom) Nine-fold coordination environment around the neodymium center. For clarity, only half of the disordered water molecules has been shown (except O1w).

discrete tetranuclear building block U_4O_{22}, which has been previously encountered in other uranyl phthalates. It has been described in the molecular assemblies of discrete tetramers[3b] or chains involving their connection through additional dimers.[3l] Other uranyl carboxylates also contains such a tetrameric motif.[2f,20] In **1** and **2**, the tetramers are connected to each other through an isolated lanthanide cation via a carboxylate function of the phthalate. The rare-earth center is coordinated to nine oxygen atoms and lies on the special position *2f*. Two of them are from the carboxylate function (Ce−O11b = 2.531(10) Å; Nd−O11b = 2.531(7) Å) and the seven remaining oxygen atoms are in terminal position. They have been assigned to aquo species, with Ce-Ow in the range 2.40(3)−2.66(3) Å in **1** and Nd-Ow in the range 2.439(15)−2.579(19) Å in **2** (Figure 1). In fact, six of the water molecules are disordered on two positions, probably because of its large location freedom around the rare earth atom. It results in a 9-fold coordination defined in a tricapped trigonal prismatic polyhedron. One of the two crystallographically independent phthalate groups plays the role of bridge between the uranyl tetramers and the lanthanide cations through one carboxylate arm, which acts as *syn-anti* bidentate linker. The second carboxylate group is linked to two uranyl centers with chelating and bidentate bridging modes (configuration: μ_5-η_1:η_2:η_1:η_1). The second phthalate species has almost the same bridging fashion but does not bond the neodymium cation. It results in a terminal C═O bond (C1a═O12a = 1.27(2) Å for **1** and 1.221(16) Å for **2**) leading to a monodentate mode, and this phthalate linker adopts a configuration μ_4-η_1:η_2:η_1. The association of the tetrameric unit with the lanthanide cation induces the formation of anionic ribbons $[(UO_2)_4O_2Ln(H_2O)_7(1,2\text{-bdc})_4]^-$ developing along the [201] direction (Figure 2). The chains are isolated to

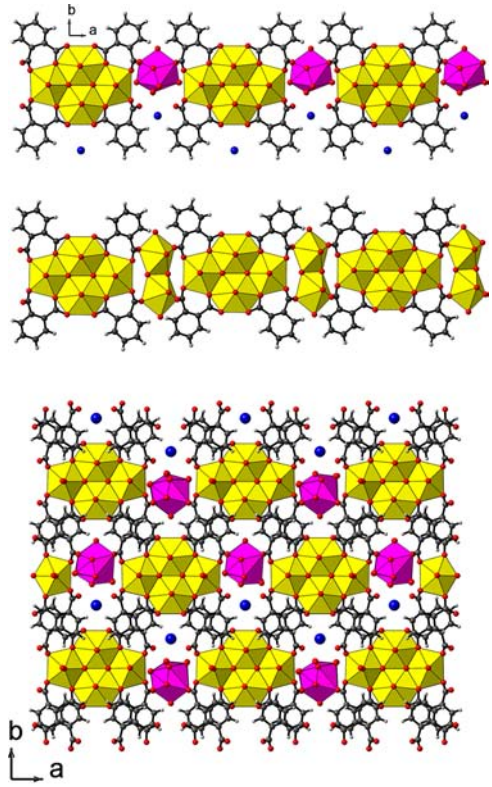

Figure 2. Structure of $(UO_2)_4O_2Ln(H_2O)_7(1,2\text{-bdc})_4{\cdot}NH_4{\cdot}xH_2O$ (Ce(**1**), Nd(**2**); x = 1 for **1**, x = 0 for **2**). (top) View of a chain running along the *a* axis, showing the alternation of uranyl-centered tetranuclear blocks (yellow) and discrete lanthanide-centered polyhedra (purple). (middle) View a chain in the uranyl phthalate[3l] $(UO_2)_3O(OH)(H_2O)(1,2\text{-bdc})_2{\cdot}A$ (A = NH_4, K). (bottom) View of the assembly of **1** in the (*a*,*b*) plane showing the ammonium cations (blue circles) intercalated between the chains.

each other by ammonium cations, which compensate its negative charges (Figure 2). Hydrogen bond interactions occur in the (*a*,*b*) plane between ammonium groups and terminal water molecules attached to lanthanide atoms (N1···O3w = 2.68(4) Å for **1**; N1···O3w = 2.82(2) Å for **2**) as well as the oxygen atoms from uranyl U2 (N1···O82a = 3.02(3) Å for **1**, N1···O82a = 3.02(2) Å for **2**). On the opposite, terminal water molecule O1w is also hydrogen bonded to O82b with a distance of 2.68(2) Å (**1**) or 2.704(10) Å (**2**). The three-dimensional cohesion is ensured by van der Waals interactions between the organic parts along the *c* axis. For the cerium-based compound (**1**), free water molecules (O5w) have been revealed by single-crystal XRD analysis and are located between the chains, with preferential hydrogen bond interactions with terminal uranyl-type oxo groups (O5w···O2u = 2.80(3) Å, O5w···O31u = 2.92(3) Å). It is interesting to notice that the structures of **1** and **2** are closely related to those of the pure uranyl phthalates[3l] $(UO_2)_3O(OH)(H_2O)(1,2\text{-bdc})_2{\cdot}A$ (A = NH_4, K). Both compounds are composed of infinite chains (Figure 2). In the previous uranyl phthalate, the tetrameric blocks are connected to each other via dimeric unit U_2O_{12}. In

dx.doi.org/10.1021/ic3005757 | *Inorg. Chem.* 2012, 51, 9610−9618

phases **1** or **2**, the uranyl dimer is substituted by one lanthanide center, which allows the connection through one carboxylate arm of the phthalate, the second being in a chelating and bidentate mode, with uranyl centers of the tetrameric block.

*Crystal Structure of $(UO_2)_3Ln_2(H_2O)_{12}(btec)_3{\cdot}5H_2O$ (Ln = Ce(**3**), Nd(**4**))*. The coordination polymer obtained from the pyromellitate linker is three-dimensional. Its asymmetric unit (Figure 3) contains two crystallographically independent

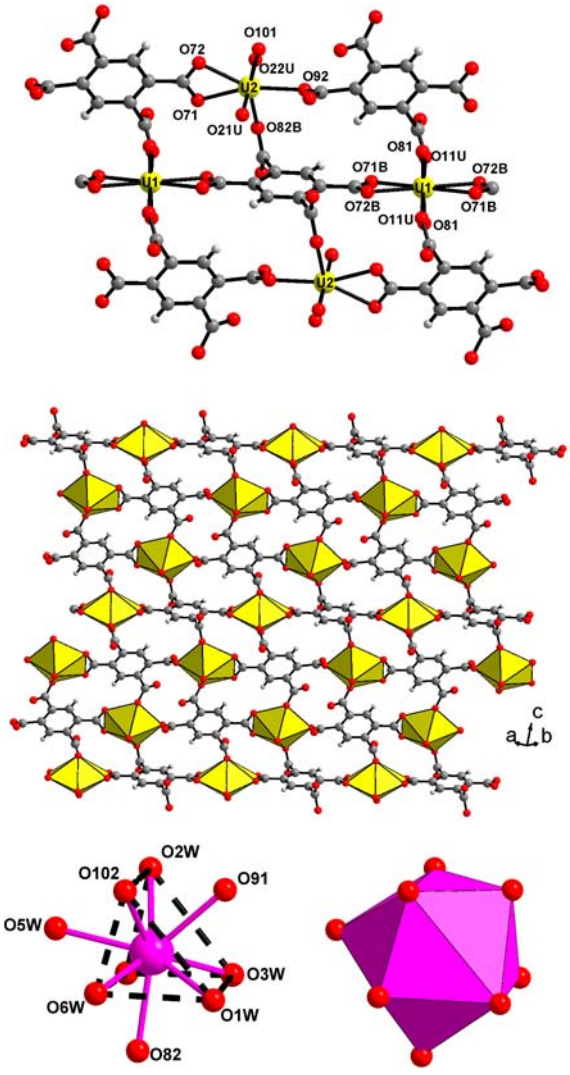

Figure 3. Structure of $(UO_2)_3Ln_2(H_2O)_{12}(btec)_3{\cdot}5H_2O$ (Ce(**3**), Nd(**4**)). (top) Representation of the two uranyl environments (hexagonal bipyramid for U1 and pentagonal bipyramid for U2). (middle) View of layer showing the connection of the two types of discrete uranyl-centered polyhedra via the pyromellitate ligands. (bottom) Coordination surrounding of the lanthanide center $LnO_2(H_2O)_7$, defining a tricapped trigonal prism. Only the Nd surrounding is represented since the Ce atom statistically lies on two sites (see Supporting Information).

uranium sites (U1 and U2), lying on the positions *1g* and *2i* and one lanthanide cation (*2i*). Uranium U1 is 8-fold coordinated (hexagonal bipyramid) whereas uranium U2 is 7-fold coordinated (pentagonal bipyramid). Typical uranyl bonds are found in the range 1.764(5)−1.780(4) Å for **3** and 1.751(5)−1.770(4) Å for **4**. Carboxyl oxygen atoms complete the coordination sphere of each uranyl center and are located in the equatorial plane. U−O distances are ranging from 2.404(4) up to 2.573(4) Å (**3**) and 2.396(3) up to 2.598(4) Å (**4**) for U1, and from 2.339(5) up to 2.455(4) Å (**3**) and from 2.338(5) up to 2.450(4) Å (**4**) for U2. The two types of uranyl cations are linked to each other via two crystallographically independent pyromellitate ligands. One of the organic molecules links the hexagonal bipyramids (U1) in a chelating bridging mode with a trans connection sequence (1,4-position) along the [1−10] direction (Figure 3). The remaining carboxylate arms (2,5-position) are bonded to pentagonal bipyramids (U2) in a monodentate manner, one C−O bond remaining free (C8b−O81b = 1.230(9) Å for **3** and 1.234(9) Å for **4**). The second pyromellitate species also connects the uranyl centers U2 to each other, via chelating and monodentate bridging modes (1,4-position) and the uranyl centers U1 in monodentate bridging modes (2,5-position). The remaining C−O bonds are attached to the lanthanide cations, and this results in a hexadentate linker for this pyromellitate species. The latter has one chelating (CO-U-OC) and three *syn-anti* bidentate (CO-U and CO-Ln) bridging modes. The other pyromellitate species acts as tetradentate linker and is only connected to uranyl centers. It results in the formation of corrugated sheets of uranyl-pyromellitate developing along the (110) plane (Figure 4), which are stacked along the [110]

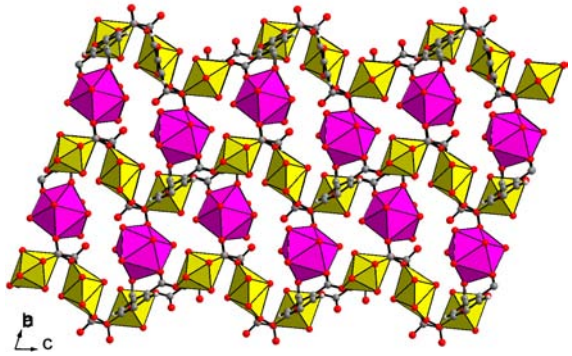

Figure 4. View along [-110] of the structure of $(UO_2)_3Ln_2(H_2O)_{12}(btec)_3{\cdot}5H_2O$ (Ce(**3**), Nd(**4**)), showing the stacking of corrugated sheets of uranyl-centered polyhedra intercalated by lanthanide-centered polyhedra.

direction through the discrete lanthanide centers. They are connected to three carboxyl oxygen atoms and six water molecules (in terminal position), defining a tricapped trigonal prismatic environment. Ce−O distances are in the range 2.497(4)−2.631(7) Å and Nd−O distances are in the range 2.432(4)−2.576(6) Å, as expected for cerium and neodymium, respectively. As previously explained (see single-crystal X-ray diffraction part), the cerium center is located on two close crystallographic positions with a statistical occupancy of 0.875(2)/0.125(2). The resulting three-dimensional network (Figure 4) exhibits some space nearby the lanthanide cations, where free water molecules are located. The latter are hydrogen bonded with the terminal aquo ligands attached to the lanthanide cations.

*Crystal Structure of $(UO_2)_2(OH)Ln(H_2O)_7(mel){\cdot}5H_2O$ (Ln = Ce(**5**), Nd(**6**))*. The structures of **5** and **6** are isomorphous and built up from the connection of uranyl-centered dinuclear units with lanthanide cations, through the mellitate linker. There are two crystallographically independent uranium atoms (U1 and U2), exhibiting identical pentagonal bipyramidal environments

dx.doi.org/10.1021/ic3005757 | *Inorg. Chem.* 2012, 51, 9610−9618

(Figure 5). As expected, two short terminal U−O bondings are found with U═O distances in the range 1.763(6)−1.782(6) Å

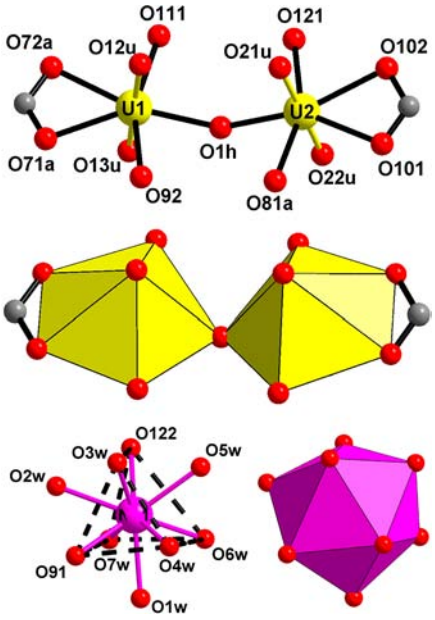

Figure 5. Structure of $(UO_2)_2(OH)Ln(H_2O)_7(mel)\cdot 5H_2O$ (Ce(**5**), Nd(**6**)). (top) Asymmetric unit showing the two 7-fold coordinated uranyl centers (pentagonal bipyramid) bridged through μ_2-OH (O1h). (bottom) Nine-fold coordination environment of the lanthanide center defining a tricapped trigonal prism.

for **5** and 1.766(5)−1.789(5) Å for **6**. For each uranium, the equatorial atoms correspond to four carboxyl oxygens (U−O = 2.358(6)−2.499(5) Å for **5**; U−O = 2.354(5)−2.493(5) Å for **6**). The remaining oxygen atom is assigned to a hydroxo group and corner-shared between the two uranyl centers. The U1−O1h and U2−O1h distances, which are slightly shorter, are 2.309(5) (**5**) and 2.303(5) Å (**6**) and 2.301(5) (**5**) and 2.293(5) Å (**6**), respectively. Corresponding bond valence calculations[19] give values of 1.23 for **5** and 1.24 for **6** and agree with the assignment of this hydroxo group. The resulting dinuclear units $U_2O_{12}(\mu_2\text{-OH})$ are further connected to each other via the carboxylate groups of mellitate, which act as chelate (× 2), bidentate (× 2), or monodentate (× 2) bridging mode. One C−O bond of the two monodentate arms is terminal with distances in the range 1.210(10)−1.266(10) Å for **5**, and 1.237(9)−1.251(9) Å for **6**. The bidentate arms are bridging one uranyl cation with one lanthanide cation. The existence of such corner-shared dimer of 7-fold coordinated uranyl is quite rare since edge-sharing connection mode is usually reported in literature. To our knowledge, there are some illustrations of such μ_2-OH dinuclear units in uranyl oxalates[21] or mixed uranyl-zinc dipicolinate-acetate.[22] The connection of the uranyl dimeric units with the mellitate molecules is developed in the (*a*,*b*) plane and generates layers, which are linked via discrete lanthanide cation (Figure 6). The latter is 9-fold coordinated to two carboxyl oxygen atoms and seven water molecules in terminal positions. The coordination environment $LnO_2(H_2O)_7$ defines a tricapped trigonal prism with Ce−O distances of 2.442(6)−2.499(6) Å and Nd−O distances of 2.442(5)−2.456(6) Å, Ce-Ow distances in the range 2.492(12)−2.590(6) Å and Nd-Ow distances in the range 2.451(13)−2.550(7) Å. In this structure, each mellitate species acts as octadentate linker, connecting six uranyl and two

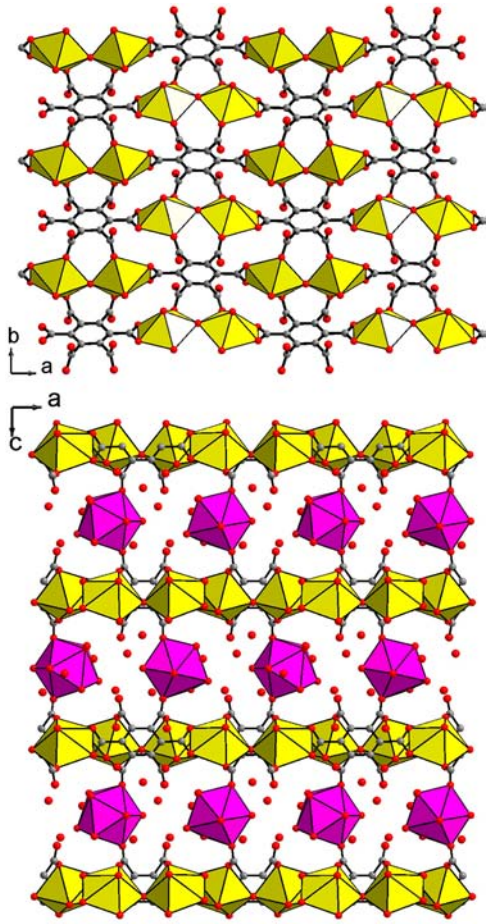

Figure 6. Structure of $(UO_2)_2(OH)Ln(H_2O)_7(mel)\cdot 5H_2O$ (top) view in the (*a*,*b*) plane, of the layer of uranyl dimeric units connected to each other through the mellitate ligands. (bottom) View along the *b* axis, showing the connection of the uranyl-based sheets with isolated lanthanide-centered polyhedra.

lanthanide centers. Between the uranyl-based layers, some free water molecules are also located and hydrogen bonded to other terminal aquo species or oxygen atoms from monodentate carboxylate groups.

Structural Discussion. One of the structural features of these different mixed uranyl-lanthanide coordination polymers lies on the existence of uranyl networks (isolated building unit, or mixed uranyl-organic layer) linked to each other through discrete lanthanide polyhedra centers. In each case, the connection between the 4f-5f elements is ensured by two or three bidentate carboxylate arms from the organic molecules. The lanthanide cations are therefore surrounded by seven or six water molecules, which do not further participate to the condensation scheme of the final network. A similar observation was reported in the previous example of mixed uranyl-lanthanide assembly $(UO_2)Ln(H_2O)_7(HL)\cdot H_2O$ (Ln = Pr, Eu, Tb, Er)[4] with the aliphatic derivative of the mellitate ligand. The occurrence of monomeric lanthanide species with high hydration state (6 or 7 H_2O) seems to be a characteristic in this class of heterometallic coordination complexes. The second aspect concerns the U/Ln ratio, which also depends on the nature of the organic ligand and the uranyl oligomer size. It is 4U/1Ln (based on tetrameric blocks in **1** and **2**), 1.5U/1Ln (based on discrete hexagonal and pentagonal bipyramids in **3** and **4**), 2U/1Ln (based in dimeric blocks in **5** and **6**), and 1U/

dx.doi.org/10.1021/ic3005757 | *Inorg. Chem.* 2012, 51, 9610−9618

1Ln (based in discrete hexagonal bipyramid[4]). Uranyl cations are known to condense upon hydrolysis to generate different oligomeric species, with the formation of di-, tri-, or tetranuclear centers.[23] From the crystal chemistry point of view, these different motifs are observed in the final coordination assemblies, but higher condensed polynuclear blocks (containing six[24] or eight[5m] uranyl centers) or ribbon-like motifs are also encountered,[21c,25] and could result from the condensation of low nuclearity uranyl oligomers. However, considering the reaction pH range (0.9−3.5), it was reported that lanthanide cations could also undergo hydrolysis reaction since formation of precipitate appears above pH 6 in aqueous solution.[26] In fact, lanthanide cations (in compounds **1**−**6**) are surrounded by solvation water species, and their coordination sphere are completed only by two or three carboxyl oxo ligands, which would correspond to the first steps of water exchange reactions with the multidentate carboxylic acids. In the presence of uranyl cations, further condensation processes (to form higher nuclearity building unit) seem to be stopped for lanthanide cations in these cases, although highly condensed building unit occurs in pure lanthanide carboxylates (see MOF-type compounds for instance).

Another type of heterometallic U-Ln assembly was also reported with the organic linker mellitate, $(UO_2)_2Ln(OH)(H_2O)(mel)_2$ (Ln = Ce, Ln) in our group.[5] These compounds were hydrothermally synthesized at 200 °C and their structures consist of direct bondings via oxo (cation−cation interaction) and hydroxo bridging ligands between uranyl and lanthanide centers. In this particular case, it seems that the reaction temperature has a drastic role for the crystallization of the different phases: lower temperature (150 °C) favored the formation of uranyl networks intercalated by isolated lanthanide cations, through carboxylate (**5**, **6**) whereas higher temperature (200 °C) gave rise to the formation of more condensed networks with the occurrence of direct U−O−Ln bonding.[5]

Thermal Behavior. The different mixed uranyl-lanthanide phases have been characterized by thermogravimetric analysis and in situ X-ray thermodiffraction (up to 800 °C) and then ex-situ X-ray diffraction for calcined product up to 1400 °C (or 1500 °C for **1** and **2**). Examples of illustrations of the thermal behavior are given for compounds **3**−**4** (Figures 7 and 8).

Thermogravimetric curves of **1** and **2** showed several loss events (see Supporting Information S5a). For **1**, up to 210 °C, three steps were observed (obs.: 1.3% at 75 °C, 1.7% at 110°C and 2.8% at 210 °C), which could be assigned to the successive departures of the free and bonded water species from the lanthanide center (calc.: 1.7% for $2H_2O$; calc.: 2.6% for $3H_2O$). The organic ligand started to be removed from 300 °C up to 470 °C. The final remaining loss was 63.9% and in good agreement with the formation of stoichiometric mixture $(4/3)U_3O_8$ and CeO_2 (calc.: 62.5%). For **2**, up to 200 °C, two steps were observed (obs.: 3.9% at 110 °C and 2.2% at 200 °C), which could be assigned to the successive departures of the bonded water species from the lanthanide center (calc.: 3.5% for $4H_2O$; calc.: 2.6% for $3H_2O$). The organic ligand started to be removed from 340 °C up to 430 °C. The final remaining loss was 62.9% and in good agreement with the formation of stoichiometric mixture $(4/3)U_3O_8$ and $(1/2)Nd_2O_3$ (calc.: 62.8%). The evolution of the X-ray diffraction patterns as a function of temperature was quite similar for both compounds **1** and **2** (Supporting Information S6a). The Bragg peaks of **1** and **2** were visible up to 200 °C and then only low angle peaks

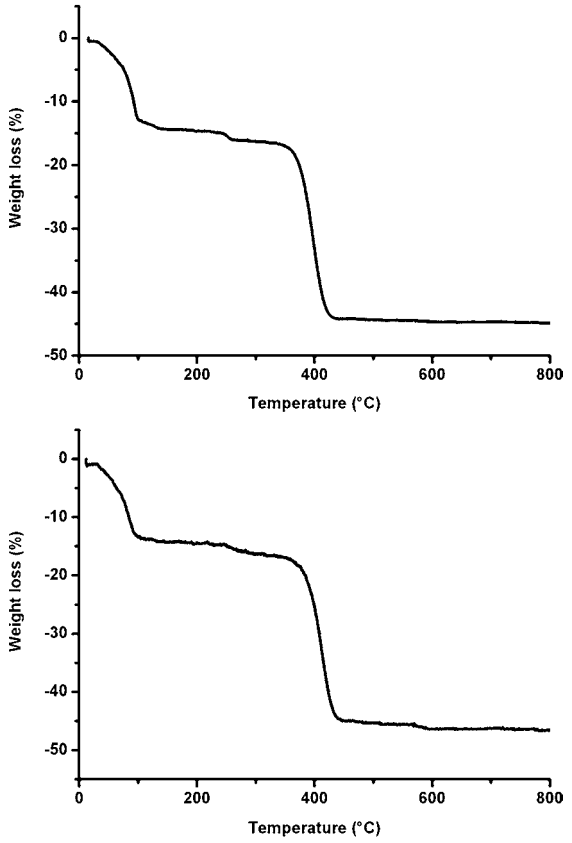

Figure 7. Thermogravimetric curves of compounds **3** (left) and **4** (right) under air atmosphere (rate 5 °C/min).

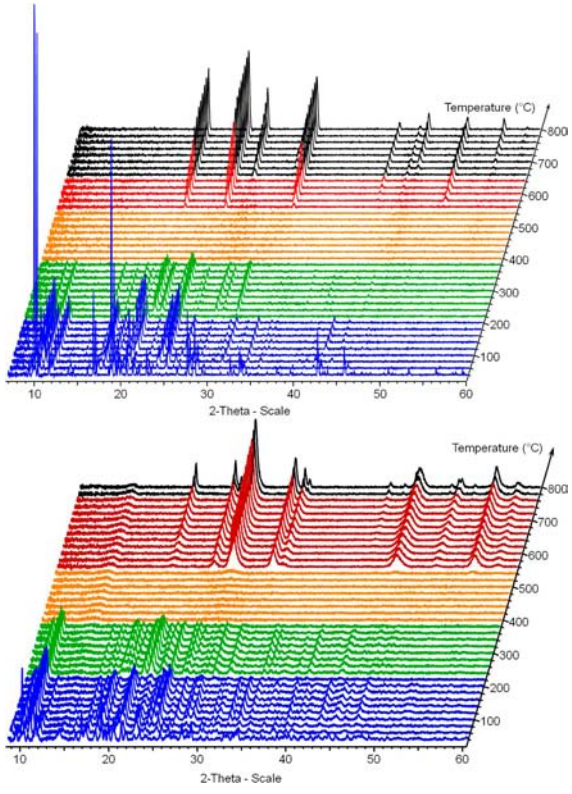

Figure 8. X-ray thermodiffractograms of $(UO_2)_3Ln_2(H_2O)_{12}(btec)_3{\cdot}5H_2O$ (Ln = Ce(**3**, top), Nd(**4**, bottom); copper radiation) under air atmosphere.

dx.doi.org/10.1021/ic3005757 | *Inorg. Chem.* 2012, 51, 9610−9618

are observed up to 340 °C. The phases are then transformed into amorphous products, which are then followed by the crystallization of uranium oxide α-UO_3 (pdf file 31-1416) up to 800 °C. A structural transformation into α-U_3O_8 (pdf file 31-1424) started from 780 °C for the solid **2**. Calcination at 1400 °C of the samples **1** and **2** led to the crystallization of a mixture of a small amount of α-U_3O_8 (pdf file 31-1424) together with $(U,Ce)O_2$ (from **1**) or $(U,Nd)O_{2-\delta}$ (from **2**) with the fluorite structure-type, as major phase. At 1500 °C, only the fluorite type phase is visible by XRD. Inductively coupled plasma (ICP) chemical elementary analysis gave the compositions $U_{0.77}Ce_{0.23}O_2$ or $U_{0.79}Nd_{0.21}O_{2-\delta}$, respectively. These values were similar to those of the expected U/Ln ratio observed in the crystal structures of the heterometallic phthalates, which gave a composition of "$U_{0.8}Ln_{0.2}$".

For compounds **3** and **4**, the thermogravimetric curve (Figure 7) showed two main weight losses. The first event occurring below 150 °C (obs.: 14.4% for **3**, 14.2% for **4**) was assigned to the departure of free encapsulated water species ($5H_2O$; calc.: 4.2% for **3** and **4**) and bonded water ($12H_2O$; calc.: 10.0% for **3** and **4**). The removal of the organic part was observed from 300 °C up to 440 °C (obs.: 27.8%; calc.: 30.4% for **3**, obs.: 28.3%; calc.: 31.1% for **4**). For **3**, the remaining weight was 55.1% and agreed well with the theoretical value (55.3%) corresponding to the mixture of U_3O_8 and $2CeO_2$. For **4**, the remaining weight was 53.6% and is close to the calculated value (54.7%) attributed to the stoichiometric mixture of U_3O_8 and Nd_2O_3. Upon heating, the X-ray diffraction patterns of both compounds **3** and **4** (Figure 8), indicated that the phases were visible up to 200 °C and some Bragg peaks persisted up to 400 °C. They are then transformed into amorphous products. From 560 °C, it appeared the crystallization of U_3O_8 (pdf file 74-562) for the mixed U−Ce solid or α-U_3O_8 (pdf file 31-1424) for the U−Nd solid, together with $(U,Ce)O_2$ or $(U,Nd)O_{2-\delta}$ with the fluorite structure type. For the Nd-based solid, a solid state transition was also observed for the uranium oxide with the structural transformation into α'-U_3O_8 (pdf file 31-1425) from 780 °C. Calcination at 1400 °C of the samples **3** and **4** led to the crystallization of one unique phase $(U,Ce)O_2$ (from **3**) or $(U,Nd)O_{2-\delta}$ (from **4**) with the fluorite structure-type. ICP elementary chemical analysis gave the compositions $U_{0.57}Ce_{0.43}O_2$ or $U_{0.55}Nd_{0.45}O_{2-\delta}$, respectively. These values were quite close to the expected ones from the starting U/Ln ratio (3/2) of the crystal structure of the heterometallic pyromellitates.

The thermogravimetric measurements of compounds **5** and **6** (see Supporting Information S5b) indicated a continuous weight loss up to 210 °C with different events. The first step could be assigned to the departure of free water (below 90 °C, obs.: 7.8%; calc. 7.2% for **5**; 7.0%; below 105 °C, calc. 7.2% for **6**) and the following loss could be assigned to water species bonded to the lanthanide center (obs.: 8.2%; calc. 10.1% for **5**; obs.: 8.3%; calc. 10.1% for **6**). The decomposition of the organic linker was visible between 320 and 450 °C (obs.: 22.4%; calc. 23.9% for **5**; obs.: 25.2%; calc. 24.5% for **6**). At 800 °C, the observed remaining weight (59.2%) based on the mixture of $(2/3)U_3O_8$ and CeO_2 for **5** was in good agreement with calculated one (58.8%). For **6**, the observed remaining weight (58.9%) based on the stoichiometric mixture of $(2/3)U_3O_8$ and $(1/2)Nd_2O_3$ was in good agreement with calculated one (58.5%). The X-ray thermodiffraction showed Bragg peaks of the compound **5** up to 200 °C, with intensities change from 40 °C, which could be correlated to the departure of encapsulated water molecules (Supporting Information S6b). After its degradation, two distinct oxides crystallized from 500 °C, and corresponded to the formation of uranium oxide α-UO_3 (pdf file 31-1416) together with a cerium−uranium oxide with the fluorite type. At 1400 °C only the mixed fluorite phase $(Ce,U)O_2$ was visible. The X-ray thermodiffraction diagram of the compound **6** was quite similar to that of its cerium analogue. The X-ray thermodiffraction showed Bragg peaks of the compounds **6** up to 200 °C, with intensities change from 40 °C, which could be correlated to the departure of encapsulated water molecules. After 200 °C, the compound was decomposed into amorphous product and then transformed into α-UO_3 (pdf file 31-1416) from 580 °C. From 710 °C, the crystallization of a second phase was observed and assigned to a neodymium−uranium oxide with the cubic fluorite type. At 1400 °C only the mixed fluorite phase $(Nd,U)O_{2-\delta}$ was visible. The formation of the fluorite-type phase is shifted to 710 °C for the Nd-based solid whereas it appeared from 500 °C for the Ce-based solid. ICP elementary chemical analysis gave the compositions $U_{0.67}Ce_{0.33}O_2$ or $U_{0.62}Nd_{0.38}O_{2-\delta}$, respectively. These values were in good agreement with the expected ones from the starting U/Ln ratio (2/1) of the crystal structure of the heterometallic mellitates.

SEM photographs (Supporting Information) of the different calcined products from compounds **1**−**6** were quite similar. They showed the crystal growth of flat domains of fluorite type phase from the crystallites of the hybrid precursors. Identical observations were previously reported in other uranyl-lanthanide mellitates.[5]

CONCLUSION

This contribution dealt with the synthesis and structural characterization of different heterometallic uranyl-cerium or uranyl-neodymium coordination complexes involving three distinct aromatic carboxylates (phthalate, pyromellitate, or mellitate). In this series, their crystal structures are built from uranyl-centered blocks (tetrameric, dimeric, or monomeric unit), linked through the carboxylate molecules and isolated lanthanide centers. The latter play the role of bridging species between the uranyl-organic networks via two or three oxygen atoms from the bidentate connection modes of the carboxylate arms of organic molecules. The coordination of the lanthanide is completed by six of seven terminal aquo species. Such a condensation mode between uranyl and lanthanide cations was previously encountered in another heterometallic multidentate carboxylate.[4] From these different cases, one invariant parameter is the existence of pairs of neighboring carboxylate groups (1,2- or 4,5- or 1,2,3,4,5,6-positions), which seems to be a key point for the assembly of uranyl and lanthanide cations. The thermal decomposition of the various coordination complexes led to the formation of mixed uranium-lanthanide oxide, with the fluorite-type structure at 1500 °C for **1**, **2** or 1400 °C for **3**−**6**. Expected U/Ln ratio from the crystal structures were observed for the calcined mixed oxide compounds **1**−**6**.

ASSOCIATED CONTENT

Supporting Information

SEM images of **1**−**6**, powder XRD patterns of **1**−**6**, crystallographic data for **1**−**6** (cif files), IR and fluorescence spectra of **1**−**6**, TG curves of **1**, **2**, **5**, **6**, X-ray thermodiffraction for **1**, **2**, **5**, **6**, SEM images and powder XRD patterns of

dx.doi.org/10.1021/ic3005757 | Inorg. Chem. 2012, 51, 9610−9618

calcined products **1**−**6**. This material is available free of charge via the Internet at http://pubs.acs.org.

AUTHOR INFORMATION

Corresponding Author

*E-mail: thierry.loiseau@ensc-lille.fr. Phone: (33) 3 20 434 434. Fax: (33) 3 20 43 48 95.

Notes

The authors declare no competing financial interest.

ACKNOWLEDGMENTS

The authors would like to thank the GNR MATINEX of PACEN interdisciplinary program and the French ANR project no. ANR-08-BLAN-0216-01 for financial support. They also would like to thank Pr. Francis Abraham and Dr Pascal Roussel for helpful discussions, Mrs. Nora Djelal and Laurence Burylo for her technical assistance with the SEM images, TG and powder XRD (UCCS). The "Fonds Européen de Développement Régional (FEDER)", "CNRS", "Région Nord Pas-de-Calais" and "Ministère de l'Education Nationale de l'Enseignement Supérieur et de la Recherche" are acknowledged for funding of X-ray diffractometers.

REFERENCES

(1) (a) Leciejewicz, J.; Alcock, N. W.; Kemp, T. J. *Struct. Bonding (Berlin)* **1995**, *82*, 43. (b) Wang, K.-X.; Chen, J.-S. *Acc. Chem. Res.* **2011**, *44*, 531. (c) Cahill, C. L.; de Lill, D. T.; Frisch, M. *CrystEngComm* **2007**, *9*, 15.

(2) (a) Bombieri, G.; Benetollo, F.; Del Pra, A.; Rojas, R. M. *J. Inorg. Nucl. Chem.* **1979**, *41*, 201. (b) Benetollo, F.; Bombieri, G.; Herrero, J. A.; Rojas, R. M. *J. Inorg. Nucl. Chem.* **1979**, *41*, 195. (c) Borkowski, L. A.; Cahill, C. L. *Inorg. Chem.* **2003**, *42*, 7041. (d) Kim, J.-Y.; Norquist, A. J.; O'Hare, D. *Dalton Trans.* **2003**, 2813. (e) Borkowski, L. A.; Cahill, C. L. *Cryst. Growth Des.* **2006**, *6*, 2241. (f) Borkowski, L. A.; Cahill, C. L. *Cryst. Growth Des.* **2006**, *6*, 2248. (g) Borkowski, L. A.; Cahill, C. L. *Acta Crystallogr., Sect. E* **2005**, *61*, m816. (h) Thuéry, P.; Masci, B. *Cryst. Growth Des.* **2008**, *8*, 3430. (i) Thuéry, P. *Cryst. Growth Des.* **2011**, *11*, 2606. (j) Thuéry, P. *CrystEngComm* **2009**, *11*, 232.

(3) (a) Charushnikova, I. A.; Krot, N. N.; Starikova, Z. A. *Radiochem.* **2004**, *46*, 556. (b) Charushnikova, I. A.; Krot, N. N.; Polyakova, I. N.; Makarenkov, V. I. *Radiochem.* **2005**, *47*, 241. (c) Liao, Z.-L.; Li, G.-D.; Wei, X.; Yu, Y.; Chen, J.-S. *Eur. J. Inorg. Chem.* **2010**, 3780. (d) Xia, Y.; Wang, K.-X.; Chen, J.-S. *Inorg. Chem. Commun.* **2010**, *13*, 1542. (e) Liao, Z.-L.; Li, G.-D.; Bi, M.-H.; Chen, J.-S. *Inorg. Chem.* **2008**, *47*, 4844. (f) Go, Y. B.; Wang, X.; Jacobson, A. J. *Inorg. Chem.* **2007**, *46*, 6594. (g) Cousson, A.; Stout, B. E.; Necroux, E.; Pagès, M.; Gasperin, M. *J. Less-Common Met.* **1986**, *125*, 111. (h) Ji, C.; Li, J.; Zheng, H. *Inorg. Chem. Commun.* **2010**, *13*, 1340. (i) Borkowski, L. A.; Cahill, C. L. *Acta Crystallogr., Sect. E* **2004**, *60*, m198. (j) Thuéry, P. *CrystEngComm* **2009**, *11*, 1081. (k) Thuéry, P. *Cryst. Growth Des.* **2011**, *11*, 347. (l) Mihalcea, I.; Henry, N.; Loiseau, T. *Cryst. Growth Des.* **2011**, *11*, 1940. (m) Mihalcea, I.; Henry, N.; Clavier, N.; Dacheux, N.; Loiseau, T. *Inorg. Chem.* **2011**, *50*, 6243. (n) Mihalcea, I.; Henry, N.; Volkringer, C.; Loiseau, T. *Cryst. Growth. Des.* **2012**, *12*, 526. (o) Severance, R. C.; Vaughn, S. A.; Smith, M. D.; Zur Loye, H.-C. *Solid State Sci.* **2011**, *13*, 1344. (p) Severance, R. C.; Smith, M. D.; Zur Loye, H.-C. *Inorg. Chem.* **2011**, *50*, 7931. (q) Wu, H. Y.; Wang, R. X.; Yang, W.; Chen, J.; Sun, Z. M.; Li, J.; Zhang, H. *Inorg. Chem.* **2012**, *51*, 3103.

(4) Thuéry, P. *Cryst. Growth Des.* **2010**, *10*, 2061.

(5) Volkringer, C.; Henry, N.; Grandjean, S.; Loiseau, T. *J. Am. Chem. Soc.* **2012**, *134*, 1275.

(6) (a) Leverd, P. C.; Rinaldo, D.; Nierlich, M. *J. Chem. Soc., Dalton Trans.* **2002**, 829. (b) Pons y Moll, O.; Le Borgne, T.; Thuéry, P.; Ephritikine, M. *Acta Crystallogr., Sect. C* **2001**, *57*, 392. (c) Schelter, E. J.; Veauthier, J. M.; Thompson, J. D.; Scott, B. L.; John, K. D.; Morris, D. E.; Kiplinger, J. L. *J. Am. Chem. Soc.* **2006**, *128*, 2198. (d) Thuéry, P. *CrystEngComm* **2008**, *10*, 1126. (e) Thuéry, P. *Inorg. Chem.* **2009**, *48*, 825. (f) Thuéry, P. *CrystEngComm* **2009**, *11*, 2319.

(7) Rojas, R. M.; Herrero, M. P.; Benetollo, F.; Bombieri, G. *J. Less-Common Met.* **1990**, *162*, 105.

(8) Diwu, J.; Wang, S.; Good, J. J.; DiStefano, V. H.; Albrecht-Schmitt, T. E. *Inorg. Chem.* **2011**, *50*, 4842.

(9) Knope, K. E.; de Lill, D. T.; Rowland, C. E.; Cantos, P. M.; de Bettancourt-Dias, A.; Cahill, C. L. *Inorg. Chem.* **2012**, *51*, 201.

(10) Thuéry, P. *CrystEngComm* **2012**, *14*, 3363.

(11) (a) Jhung, S. H.; Lee, J.-H.; Forster, P. M.; Férey, G.; Cheetham, A. K.; Chang, J.-S. *Chem.—Eur. J.* **2006**, *12*, 7899. (b) Haque, E.; Khan, N. A.; Par, J. H.; Jhung, S. H. *Chem.—Eur. J.* **2010**, *16*, 1046. (c) Khan, N. A.; Jhung, S. H. *Cryst. Growth. Des.* **2010**, *10*, 1860.

(12) Lhoste, J.; Henry, N.; Loiseau, T.; Abraham, F. *Inorg. Chem. Commun.* **2011**, *14*, 1525.

(13) (a) Ni, Z.; Masel, R. I. *J. Am. Chem. Soc.* **2006**, *128*, 12394. (b) Klinowski, J.; Almeida Paz, F. A.; Silva, P.; Rocha, J. *Dalton Trans.* **2011**, *40*, 321.

(14) *SAINT Plus*, Version 7.53a; Bruker Analytical X-ray Systems: Madison, WI, 2008.

(15) Sheldrick, G. M. *SADABS, Bruker-Siemens Area Detector Absorption and Other Correction*, Version 2008/1; University of Göttingen: Göttingen, Germany, 2008.

(16) Petricek, V.; Dusek, M.; Palatinus, L. *JANA2006. Structure determination software programs*; Institute of Physics: Praha, Czech Republic, 2006.

(17) Van Smaalen, S.; Palatinus, L.; Schneider, M. *Acta Crystallogr., Sect. A* **2003**, *59*, 459.

(18) Momma, K.; Izumi, F. *J. Appl. Crystallogr.* **2008**, *41*, 653.

(19) Burns, P. C.; Ewing, R. C.; Hawthorne, F. C. *Can. Mineral.* **1997**, *35*, 1551.

(20) Grigorev, M. S.; Antipin, M. Y.; Krot, N. N. *Radiochem.* **2004**, *46*, 224.

(21) (a) Thuéry, P. *Polyhedron* **2007**, *26*, 101. (b) Artemeva, M. Y.; Mikhailov, Y. N.; Gorbunova, Y. E.; Serezhkina, L. B.; Serezhkin, V. N. *Russ. J. Inorg. Chem.* **2003**, *48*, 1337. (c) Rowland, C. E.; Cahill, C. L. *Inorg. Chem.* **2010**, *49*, 6716.

(22) Jiang, Y.-S.; Li, G.-H.; Tian, Y.; Liao, Z.-L.; Chen, J.-S. *Inorg. Chem. Commun.* **2006**, *9*, 595.

(23) (a) Sylva, R. N.; Davidson, M. R. *J. Chem. Soc., Dalton Trans.* **1979**, 465. (b) Müller, K.; Brendler, V.; Foerstendorf, H. *Inorg. Chem.* **2008**, *47*, 10127. (c) Berto, S.; Crea, F.; Daniele, P. G.; Gianguzza, A.; Pettignano, A.; Sammartano, S. *Coord. Chem. Rev.* **2012**, *256*, 63.

(24) Zheng, Y.-Z.; Tong, M.-L.; Chen, X.-M. *Eur. J. Inorg. Chem.* **2005**, 4109.

(25) Rowland, C. E.; Belai, N.; Knope, K. E.; Cahill, C. E. *Cryst. Growth Des.* **2010**, *10*, 1390.

(26) Baes, C. F.; Mesmer, R. E. *The hydrolysis of Cations*; Krieger Publishing Compagny: Malabar, FL, 1986; p 129.